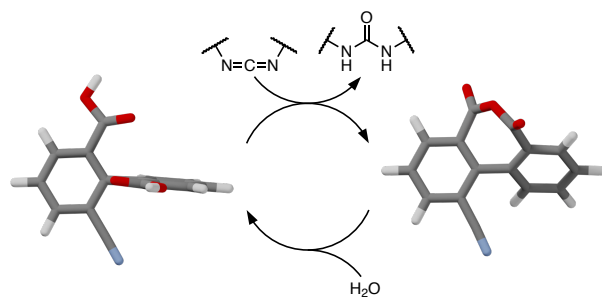# Substituent effects on transient, carbodiimide-fueled geometry changes in diphenic acids

Isuru M. Jayalath, Madelyn M. Gerken, Georgia Mantel, and C. Scott Hartley*

Department of Chemistry & Biochemistry, Miami University, Oxford, Ohio 45056, United States

Abstract

Nucleotide-fueled conformational changes in motor proteins are key to many important cell functions. Inspired by this biological behavior, we report a simple chemical system that exhibits carbodiimide-fueled geometry changes. Bridging via transient anhydride formation leads to a significant reduction of the twist about the biaryl bond of substituted diphenic acids, giving a simple molecular clamp. The kinetics are well-described by a simple mechanism, allowing structure–property effects to be determined. The kinetic parameters can be used to derive important characteristics of the system such as the efficiencies (anhydride yields), maximum anhydride concentrations, and

1

overall lifetimes. Transient diphenic anhydrides tolerate steric hindrance ortho to the biaryl bond but are significantly affected by electronic effects, with electron-deficient substituents giving lower yields, peak conversions, and lifetimes. The results provide useful guidelines for the design of functional systems incorporating diphenic acid units.

Introduction

A continuous input of energy is required for many biochemical processes.[1] These "dissipative" systems[2,3] exhibit behavior that is impossible at thermodynamic equilibrium, including cooperative sensitivity (adaptability),[4] self-production,[5] and self-healing.[6] While biology's ultimate energy source is light, chemical fuels are usually used to deliver energy to molecular systems. For example, actin-based myosin motor proteins use energy from ATP hydrolysis to slide along actin filaments, leading to muscle contraction. Likewise, and the regulation of microtubule polymerization by GTP hydrolysis leads to remarkable dynamic behavior.[7] The use of high-energy chemical species instead of light increases the complexity and specificity of these processes, affording control over their specific location, time, and extent.[8,9] Transient geometry changes are of particular significance. Many cell functions, for example, including DNA replication,[10] cell division,[11] protein transport,[12] signal transduction,[13] and active transport,[7,14] are associated with nucleotide-fueled conformational changes.

Abiotic systems that are driven out-of-equilibrium by chemical fuels have recently received a great deal of attention.[1,15–17] Carbodiimides, typically EDC ((N-(3-(dimethylamino)-propyl)-N'-ethylcarbodiimide hydrochloride), stand out as versatile fuels. They have been used in recent reports by Boekhoven,[18–20] us,[21–23] Das,[24,25] and several other research groups[26–28] to generate nonequilibrium behavior. The associated chemistry is quite simple: carbodiimides react with aqueous carboxylic acids to generate carboxylic anhydrides that then undergo hydrolysis to regenerate the parent carboxylic acids. The net result is the formation of a transient covalent bond that can be coupled to nonequilibrium behavior.[15]

In previous work,[29] we demonstrated chemically fueled geometry changes using the water-
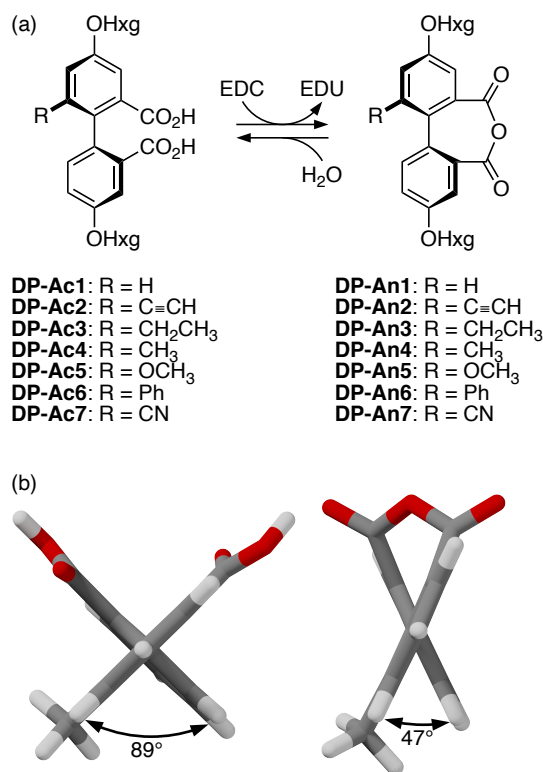
Figure 1: (a) Transient anhydride formation in diphenic acids. (b) Model acid and anhydride geometries (**DP-Ac4**/**DP-An4**, OHxg replaced with H) optimized at the B97-D3(BJ)/TZV(2d,2p) level and viewed down the biaryl axis.

soluble diphenic acids **DP-Ac1**–**DP-Ac3** in Figure 1a. On reaction with EDC, they form (intramolecular) anhydrides, giving rise to significant changes in the twist about the biaryl bond as shown in Figure 1b. In a simplistic way, this motion is similar to the clamping motion observed in ATP-binding cassette transporters, which act as pumps for active transport through cell membranes.[7,14] Of course, these biological systems involve complex aggregated macromolecules whereas the system we describe here is a single small-molecule clamp.

Our initially reported conditions worked well for unhindered diphenic acid derivative **DP-Ac1**. Since applications of these units within larger systems will require substitution, we also investigated the sterically more demanding cases **DP-Ac2** and **DP-Ac3**. Transient anhydrides were indeed generated, but the systems were not kinetically well-behaved under our original conditions, preventing analysis of structure–property effects.[29] Here, we report the expanded series of diphenic acid derivatives in Figure 1a. Suitable conditions for quantitative

mechanistic analysis of EDC-fueled anhydride formation have been identified. Substituent effects have been determined, with implications for the design of more-sophisticated systems incorporating diphenic acid subunits.
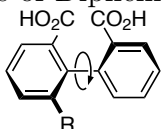
Results & Discussion

Diphenic acids **DP-Ac1**–**DP-Ac7** were designed to test both steric and electronic effects on the kinetics of formation and hydrolysis of transient anhydrides while being synthetically accessible from common intermediates.[30] Hexaglyme groups were incorporated to ensure water solubility of all species.

Gas-phase DFT geometry optimizations at the B97-D3(BJ)/TZV(2d,2p) level, summarized in Table 1, were carried out to understand the changes in geometry expected for these systems. The benzene rings of the diphenic acids are approximately orthogonal in most cases, as measured by the torsional angle (ϕ_{acid}) between the two rings, except for **DP-Ac1** (as previously reported[29]) and **DP-Ac6**. The smaller ϕ_{acid} for **DP-Ac1** (R = H) is unsurprising given that it is less sterically hindered. For **DP-Ac6** (R = Ph), it is likely due to attractive arene–arene interactions between the phenyl substituent and the opposite aromatic ring of the diphenic acid moiety. In all cases, anhydride formation bridging the two aryl rings is predicted to reduce the twist. The dihedral ($\phi_{\text{anhydride}}$) is similar for all substituted anhydrides, 6°–13° larger than for **DP-An1**. The net change $\Delta\phi$ is predicted to be about 45° for most cases except for **DP-Ac6**/**DP-An6** because of the relatively small ϕ_{acid}. Thus, we expect significant changes in twist in all of the studied systems.

Previously reported[29] **DP-Ac1**, **DP-Ac2**, and **DP-Ac3** had been prepared from key intermediates **1** and **2**, which were also used as the starting points for the syntheses of the new compounds as shown in Scheme 1. Thus, compound **1** was borylated, giving **3**, and the methyl substituent introduced via Suzuki coupling to give **4**. This intermediate was reduced (**5**), diazotized and hydrolyzed (**6**), alkylated (**7**), and saponified to obtain **DP-Ac4**

Table 1: Biaryl Dihedral Angles of Diphenic Acids and Their Anhydrides.[a]

R	ϕ_{acid}	$\phi_{\text{anhydride}}$	$\Delta\phi$
H	82°	37°	45°
CCH	91°	44°	47°
C_2H_5	91°	50°	41°
CH_3	89°	47°	42°
OCH_3	95°	44°	51°
Ph	70°	44°	26°
CN	89°	43°	47°

[a]Optimized at the B97-D3(BJ)/TZV(2d,2p) level. Calculations for H, CCH, and C_2H_5 were previously reported.[29]

(Scheme 1a). Compound **3** was also oxidized (**8**) and methylated to incorporate the methoxy substituent (**9**). The side-chains were introduced as described above to give **DP-Ac5** (Scheme 1b). A Suzuki reaction between **1** and phenylboronic acid (**13**) followed by the same set of transformations gave **DP-Ac6** (Scheme 1c). Finally, the cyano substituent was incorporated by a palladium-catalyzed cyanation reaction of **2** with zinc(II) cyanide (**17**), which was alkylated and saponified to get **DP-Ac7** (Scheme 1d).

The behavior of the seven diacid systems on treatment with EDC was then followed by ^{1}H NMR spectroscopy. In our previous work, we were unable to describe the behavior of **DP-Ac2** and **DP-Ac3** using simple kinetic models when the reactions were carried out in 7:3 D_2O:acetone-d_6 (conditions that had worked well for **DP-Ac1**). The EDC decomposition kinetics were inconsistent (faster at very early reaction times, then slowing sharply) and we observed the formation of transient byproducts that were not easily quantified. For the present work, the following changes were made to optimize the conditions for kinetics analysis. First, the proportion of acetone in the solvent was increased to 1:1 to avoid aggregation or precipitation. Second, the reaction mixtures were made more acidic by adjusting the pD of the D_2O to 2 before addition of the acetone-d_6. This minimizes the increase in pD that occurs when the concentration of diacid falls, ensuring that the remaining diacid is
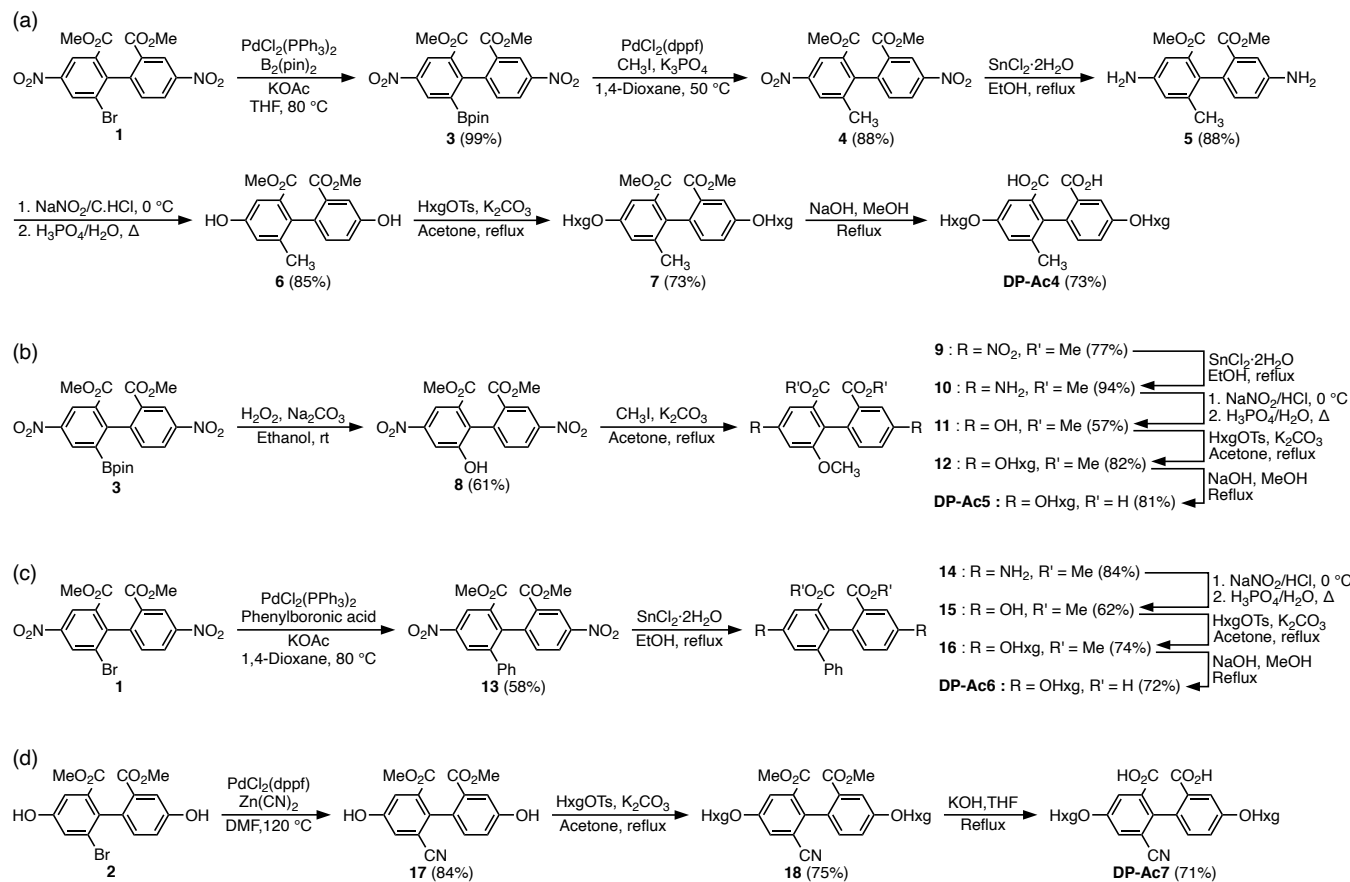
Scheme 1: Synthesis of diphenic acids (a) **DP-Ac4**, (b) **DP-Ac5**, (c) **DP-Ac6**, and (d) **DP-Ac7**.

protonated throughout the experiment and that the EDC reactivity is consistent. Finally, a small amount of pyridine-d_5 was added to minimize the formation of any unproductive intermediates due to the rearrangements of the *O*-acylisourea intermediate.[31] Kinetic runs were carried out at 276 K, ensuring a reasonable time scale. Concentrations and chemical shifts were calculated with respect to an internal standard (ethylene carbonate).

The diacids (10 mM) all react smoothly with EDC giving EDU and transient species that are clearly distinguishable in the aromatic regions of the ^{1}H NMR spectra (see full spectra in the Supporting Information). These transient species were confirmed to be the cyclic anhydrides by separately synthesizing authentic samples that were identified by mass spectrometry (see Supporting Information).

Figure 2 shows representative ^{1}H NMR spectra for typical kinetic runs of **DP-Ac4/DP-An4** (Figure 2a) and **DP-Ac6/DP-An6** (Figure 2b). Early on, the signals assigned to the anhydrides grow with the concomitant decrease of the signals of the starting acids. Anhydride hydrolysis then dominates after several minutes. In most cases, the transient anhydride ^{1}H NMR peaks are deshielded compared to the parent acid, as is the case for **DP-Ac4/DP-An4** (Figure 2a). The spectra of the **DP-Ac6/DP-An6** system are different, in that the ^{1}H NMR peaks of **DP-An6** are generally more shielded compared to **DP-Ac6** (Figure 2b), presumably because protons on the diphenic acid core are brought into the shielding zone of the phenyl substituent as the twist is reduced (Figure 1 and Table 1). This observation confirms that significant geometry changes occur on formation of the cyclic anhydrides.

To quantify the kinetics, we performed four runs per acid (10 mM), varying the starting EDC concentration ($[EDC]_0$) from 5–20 mM (0.5–2 equiv). The concentration vs time plots were then fit to the following minimal kinetic model based on the well-known reactivity of carbodiimides with carboxylic acids and anhydride hydrolysis.[32–36] The initial reaction of a single carboxylic acid group in the diacid (DA) with EDC in the presence of pyridine should generate an acylpyridinium intermediate (I) via the *O*-acylisourea, simultaneously forming the urea EDU as a waste product (eq 1).[22,32–34] All of the substituted systems can
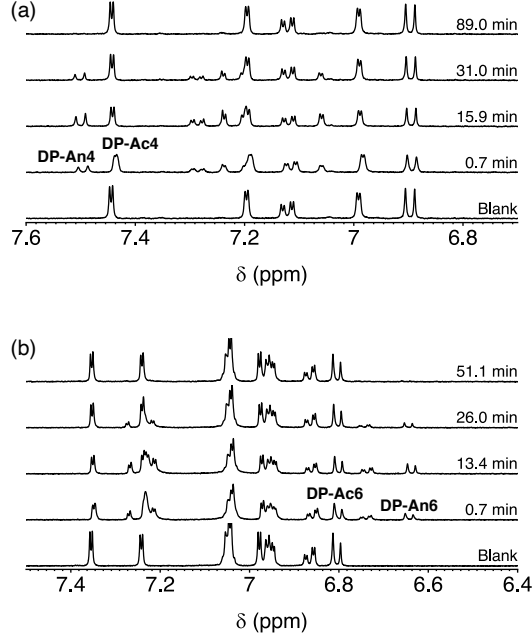
Figure 2: ^{1}H NMR spectroscopy of the treatment of (a) **DP-Ac4** and (b) **DP-Ac6** (10 mM) with EDC (1 equiv) in D$_2$O:acetone-d_6 (1:1) in the presence of pyridine-d_5 (2 mM) at 276 K (pD of D$_2$O adjusted to pD = 2 prior to mixing with the acetone).

potentially give two distinct isomers of I depending on which carbonyl reacts; for the purposes of modeling we do not distinguish these possibilities. Intermediate I can either generate the anhydride by intramolecular reaction with the other acid group (eq 2), or it can reform the starting acid by unproductive hydrolysis (eq 3). The anhydride can hydrolyze back to the starting acid via the same acylpyridinium intermediate I (eq 2).[22,35,36]

$$DA + EDC \xrightarrow{k_1} I + EDU \tag{1}$$

$$I \underset{k_2}{\overset{k_i^{An}}{\rightleftharpoons}} An \tag{2}$$

$$I \xrightarrow{k_i^{DA}} DA \tag{3}$$

Applying a steady-state approximation in I simplifies the parameters with $\alpha = \frac{k_i^{DA}}{k_i^{An}}$.

Our goal here is to describe the broad features of the system studied. Thus, the above kinetic model lacks some mechanistic details such as the pD-dependence of the rate constants
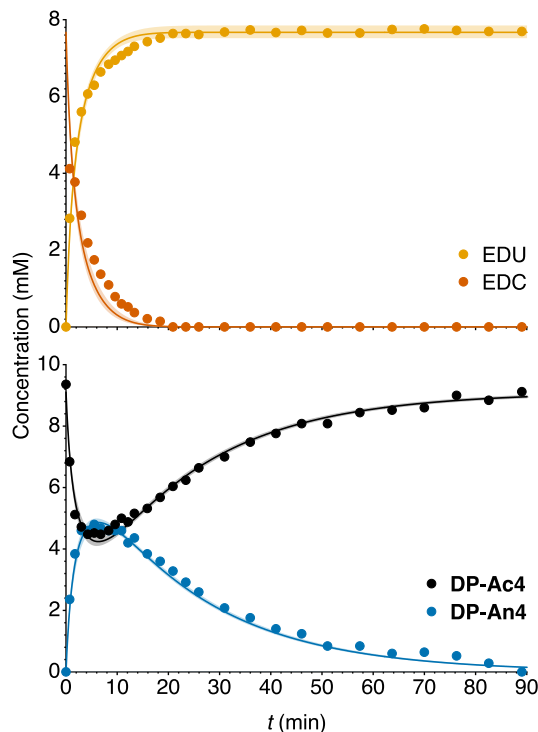
8

Figure 3: Concentration vs time for the **DP-Ac4**/**DP-An4** system with the addition of 8 mM EDC to 10 mM **DP-Ac4**. Solid lines represent the fits to the kinetic model and the shaded areas represent 95% confidence intervals for the fits (in some cases, the CIs are narrow enough to be difficult to distinguish from the line). The data from four experiments with variable $[EDC]_0$ was fit simultaneously, not just the example shown.

and EDC speciation.[37] Nevertheless, the experimental datasets are well-fit by the differential equations describing the mechanism (see Supporting Information). Figure 3 depicts a typical plot for **DP-Ac4**/**DP-An4**. Note that the fit was obtained by numerically fitting all four data sets simultaneously (i.e., not just the example shown). A non-parametric bootstrapping method was used to estimate the uncertainties of the regression (95% confidence interval).[22] The independence of the parameters was further confirmed by generating confidence contour plots as shown in the Supporting Information.[38] The parameters are well-constrained by the data for all seven substrates.

Figure 4 shows the parameters k_1, k_2, and α as a function of the Hammett constants for each substituent (σ_m).[39,40] There is no meaningful correlation between k_1, the rate of reaction of EDC with the diacid, and σ_m. The parameter k_2, which represents the rate of anhydride
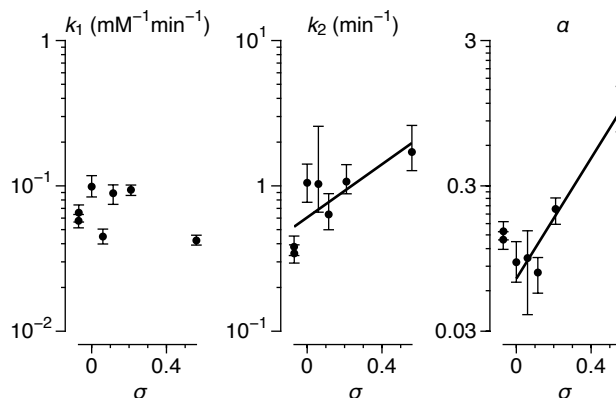
Figure 4: Dependence of kinetic parameters on σ_m. The uncertainties are 95% confidence intervals. The trend line for α does not include the two points at $\sigma_m < 0$ (see text for explanation).

decomposition, shows a weak positive correlation with σ_m. This is expected as electron-withdrawing groups have long been known to accelerate the hydrolysis of anhydrides.[41] Analogous behavior was seen for α, which represents the partitioning of the intermediate between hydrolysis and anhydride formation, implying that electron-withdrawing groups favor hydrolysis of the activated intermediate (I) over anhydride formation. This is the most significant substituent effect for these diphenic acid systems; interestingly, this was not the case in our previous work on intermolecular anhydride formation in simple substituted benzoic acids, where differences in behavior could be explained mostly in terms of the parameter analogous to k_2.[22] A close look at Figure 4 shows that changes in α level off when σ_m is less than about 0.1. It is possible that this is because the anhydrides are unsymmetrical; that is, the most electrophilic carbonyl would be preferentially attacked by pyridine, and thus attack at the unsubstituted side would be favored for electron-donating substituents, leading to little difference in behavior.

Surprisingly, attempts to include steric effects, via Taft parameters or simply the dihedrals in Table 1, did not give significant improvements to the fits for k_1, k_2, or α (see Supporting Information for analysis). The kinetics of both anhydride formation and hydrolysis are clearly not significantly affected by steric hindrance within the scope of the substituents studied here.
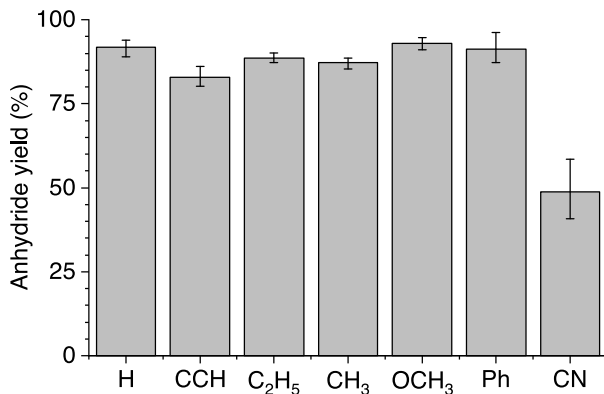
Figure 5: Yields of **DP-An1**–**DP-An7** calculated from α values.

The parameters obtained from the fits fully describe the behavior of these systems. However, it can be helpful to translate them into more easily appreciated characteristics. In conventional synthetic chemistry, reactions are often characterized by reaction yields and times. However, the "yields" of transient anhydrides in these systems is zero by definition and the reaction times depend on the specific set of starting conditions. We define instead the yields for these systems as the total amounts of anhydride generated with respect to the amount of EDC added. We also consider the peak anhydride concentration ($[\text{An}]_{\text{max}}$) and the acid recovery time (τ_{99}), defined as the time that it takes to return to 99% of the starting acid concentration.

For the simple mechanism described here, the anhydride yields are independent of the concentrations of both diacid and EDC, depending only on the partitioning of the intermediate between anhydride formation (eq 2) and hydrolysis (eq 3). They are simply $(1 + \alpha)^{-1}$ and are shown in Figure 5. Most of the diphenic acid systems are very efficient, converting about 90% of the EDC into anhydride. The exception is cyano-substituted **DP-Ac7**, with a yield of only $49^{+10}_{-8}\%$. Here the intermediate partitions evenly between activation (anhydride) and deactivation (hydrolysis) ($\alpha = 1.0^{+0.4}_{-0.3}$ for **DP-Ac7**). We conclude that, functionalizing diphenic acids with electron-withdrawing groups causes significant loss of efficiency of the system.

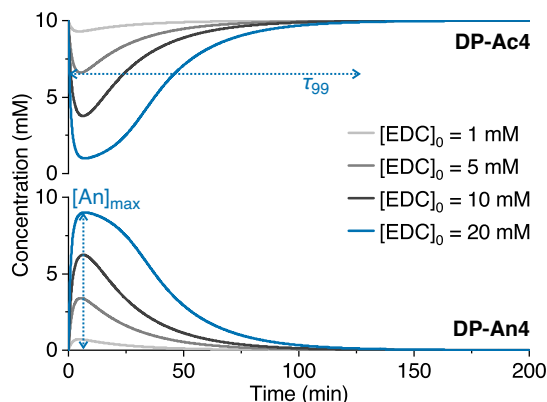The characteristics $[\text{An}]_{\text{max}}$ and τ_{99}, which measure the overall shapes of the concentration

Figure 6: Simulated behavior of 10 mM **DP-Ac4**/**DP-An4** for different EDC concentrations $[EDC]_0$.

vs time plots, can be obtained from kinetic simulations based on the experimentally determined values of k_1, k_2, and α.[22,29] Simulations were carried out for 10 mM solutions of the starting acids and variable starting concentrations of EDC ($[EDC]_0$) (0.5–50 mM). Figure 6 shows selected examples for **DP-Ac4**. The values of $[An]_{max}$ and τ_{99} extracted from these simulations are shown as a function of $[EDC]_0$ in Figure 7 (left). As expected, $[An]_{max}$ increases with increasing $[EDC]_0$, plateauing near the starting acid concentrations. The anhydride lifetimes τ_{99} initially increase rapidly with increasing $[EDC]_0$ and then increase approximately linearly, with slopes that are strongly dependent on the nature of the substituents.

Both $[An]_{max}$ and τ_{99} have a complex dependence on both k_2 and α, but there are some general trends. First, $[An]_{max}$ depends primarily on α. The plot in Figure 7a (right) shows that there is a reasonable inverse correlation between them for a given $[EDC]_0$. This is consistent with the mechanism, since the peak anhydride concentration is reached soon after treatment with EDC (e.g., Figure 6), before significant anhydride hydrolysis has occurred, and would therefore be expected to depend mostly on the distribution of the intermediate between anhydride and deactivation as it is generated directly by the EDC. As a consequence, the $[An]_{max}$ for the electron-deficient **DP-Ac7**/**DP-An7** system is much smaller than that for the others for a given $[EDC]_0$. Second, τ_{99} depends primarily on k_2. This is shown in Figure 7b (right), which shows that the slope of the linear region of the τ_{99} vs $[EDC]_0$ plots
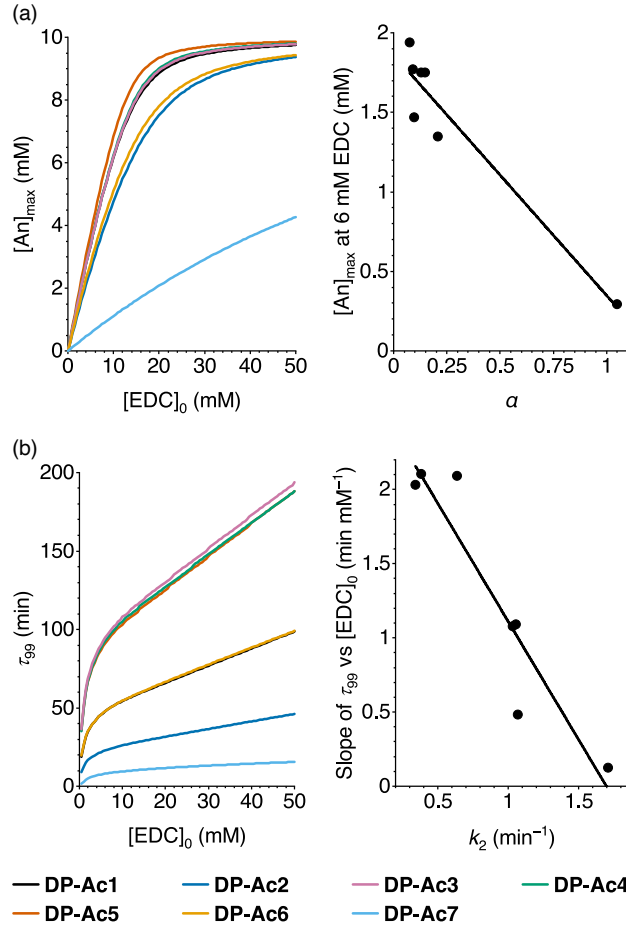
12

Figure 7: Simulated behavior of 10 mM diacids as a function of initial EDC concentration $[EDC]_0$. (a) Maximum anhydride concentration $[An]_{max}$ (left) and values extracted at 6 mM EDC vs α (right). (b) Time to recover 99% of the starting acid τ_{99} (left) and the slope of the linear region of the plots (taken from 20–50 mM) vs k_2 (right).

13

is inversely correlated with k_2. This follows from the intuitive expectation that the overall lifetime of the system derives primarily from the anhydride decomposition rate, and is shorter for electron-poor anhydrides.

These structure–property effects will be important to consider when designing more-complex systems that make use of diphenic acids for nonequilibrium geometry changes. First, the results here show that this system is tolerant of steric hindrance ortho to the biaryl bond but sensitive to electronic effects. Substitution with electron-withdrawing groups reduces the overall efficiencies, peak anhydride concentrations, and transient state lifetimes. This is consistent with the behavior of simple benzoic acids[22] but, it should be noted, there are subtle differences in the relative importance of k_2 and α.

Inspection of Figure 7 shows that the behavior of these systems tends to depend more strongly on the substituent effects than it does the fuel concentration. As a consequence, it will not generally be possible to overcome challenges in the molecular design by simply adding more fuel, as we have previously noted.[22]

Conclusions

Monosubstituted diphenic acids **DP-Ac1**–**DP-Ac7** have been synthesized and subjected to transient anhydride formation fueled by EDC. Optimization of the reaction conditions yielded kinetically well-behaved systems that are described by a simple mechanism. Within the scope of the examined substituents, the formation and decomposition of diphenic anhydrides are only weakly sensitive to steric effects but depend strongly on electronics. The overall efficiencies, as measured by the yield of anhydride relative to the EDC consumed, are generally high (roughly 90%), except for the most electron-deficient system (CN). Larger differences are observed in the maximum anhydride concentrations $[\text{An}]_{\text{max}}$ and lifetimes τ_{99}. In general, $[\text{An}]_{\text{max}}$ tends to depend primarily on α, which represents the partitioning of the acylpyridinium intermediate between anhydride formation and hydrolysis. Likewise, τ_{99} depends primarily

on the anhydride decomposition rate k_2. These diphenic acids are simple chemically fueled molecular clamps, mimicking the transient conformational changes found in biochemistry. We are currently working to apply them within systems designed for more-sophisticated nonequilibrium behavior.

Experimental Section

General Procedures

Unless otherwise noted, all starting materials, reagents, and solvents were purchased from commercial sources and used without further purification. Hexa(ethylene glycol)monomethyl ether tosylate (HxgOTs) was synthesized following a literature procedure.[42] NMR spectra for characterization were measured for $CDCl_3$ or DMSO-d_6 solutions using Bruker Avance 500 MHz or Bruker Avance NEO 400 MHz NMR spectrometers. Chemical shift values (δ) are reported in parts per million relative to tetramethylsilane. The residual $CHCl_3$ and DMSO signals were used as the internal standards for both [1]H (7.26 ppm and 2.50 ppm) and [13]C (77.16 ppm and 39.52 ppm). ^{1}H NMR spectra for kinetics were measured for D_2O/acetone-d_6 solutions using a Bruker Avance 500 MHz spectrometer and referenced to the methylene signal of the internal standard ethylene carbonate (4.50 ppm). Melting points were determined using a Thermal Analysis Q20 differential scanning calorimeter at a heating rate of 10 °C/min.

Dimethyl [1,1'-biphenyl]-6-(4,4,5,5-tetramethyl-1,3,2-dioxaborolan-2-yl)-4,4'-dinitro-2,2'-dicarboxylate (3)

A dry Schlenk vacuum tube containing dimethyl [1,1'-biphenyl]-6-bromo-4,4'-dinitro-2,2'-dicarboxylate **1** (5.00 g, 10.43 mmol), bis(pinacolato)diboron (4.50 g, 17.7 mmol), KOAc (4.6 g, 46.93 mmol), and $PdCl_2(PPh_3)_2$ (879 mg, 1.25 mmol) was evacuated and backfilled with argon (3×). To this solid mixture was added dry THF (50 mL) and the reaction mixture

was degassed by three freeze–pump–thaw cycles. The reaction mixture was then stirred and heated overnight at 80 °C, cooled to room temperature, and filtered through a Celite pad. The filtrate was diluted with EtOAc; washed with water (3×), sat. $NaHCO_3$(aq) (1×), and brine (1×); dried over $MgSO_4$; and filtered. The resulting solution was concentrated under reduced pressure and purified on a silica column eluted with 80:20 hexane:EtOAc to afford compound **3** (5.0 g, 99%) as a white solid: mp 150.94 °C; ^{1}H NMR (500 MHz, DMSO-d_6) δ 8.77 (d, J = 2.5 Hz, 1H), 8.71 (d, J = 2.4 Hz, 1H), 8.57 (d, J = 2.5 Hz, 1H), 8.44 (dd, J = 8.4, 2.5 Hz, 1H), 7.45 (d, J = 8.4 Hz, 1H), 3.65 (s, 3H), 3.62 (s, 3H), 1.01 (d, J = 15.4 Hz, 12H); ^{13}C{^{1}H} NMR (126 MHz, DMSO-d_6) δ 164.5, 164.3, 152.5, 148.3, 146.9, 146.3, 131.6, 131.4, 130.3, 130.1, 126.4, 125.9, 123.6, 84.3, 52.6, 52.5, 24.13, 24.10; HRMS (APCI-MS) calcd for $C_{22}H_{24}BN_2O_{10}$ ([M + H]$^+$) 487.1523, found 487.1520.

Dimethyl [1,1'-biphenyl]-6-methyl-4,4'-dinitro-2,2'-dicarboxylate (4)

A dry Schlenk vacuum tube containing compound **3** (3.28 g, 6.74 mmol), Pd(dppf)Cl$_2$ (493.5 mg, 0.674 mmol), and K_3PO_4 (3.60 g, 16.85 mmol) was evacuated and backfilled with argon (3×). To this solid mixture was added iodomethane (0.84 mL, 13.5 mmol) and dry 1,4-dioxane (30 mL). The reaction mixture was degassed by three freeze–pump–thaw cycles and then stirred and heated at 50 °C overnight, cooled to room temperature, and filtered through a Celite pad. The filtrate was diluted with EtOAc; washed with water (3×) and brine (1×); dried over $MgSO_4$; and filtered. The resulting solution was concentrated under reduced pressure and purified on a silica column eluted with 90:10 cyclohexane:EtOAc to afford compound **4** (2.22 g, 88%) as a pale brown solid: mp 143.06 °C; ^{1}H NMR (500 MHz, DMSO-d_6) δ 8.75 (d, J = 2.4 Hz, 1H), 8.56 (d, J = 2.5 Hz, 1H), 8.51 (dd, J = 8.4, 2.5 Hz, 1H), 8.48 (d, J = 1.7 Hz, 1H), 7.51 (d, J = 8.4 Hz, 1H), 3.66 (s, 3H), 3.60 (s, 3H), 2.03 (s, 3H); ^{13}C{^{1}H} NMR (126 MHz, DMSO-d_6) δ 164.6, 164.2, 147.03, 146.99, 146.6, 146.3, 139.2, 131.2, 129.9, 129.7, 127.6, 127.1, 124.7, 122.0, 52.7, 52.6, 20.1; HRMS (ESI-MS) calcd for $C_{17}H_{14}N_2O_8Na$ ([M + Na]$^+$) 397.0642, found 397.0641.

Dimethyl [1,1'-biphenyl]-4,4'-diamino-6-methyl-2,2'-dicarboxylate (5)

Compound **4** (2.00 g, 5.34 mmol) was dissolved in EtOH (125 mL) in a round-bottomed flask. $SnCl_2 \cdot 2H_2O$ (12.00 g, 53.4 mmol) was added and the reaction mixture was stirred and heated to reflux for 2 h then cooled to room temperature. Excess EtOH was removed under reduced pressure and sat. $Na_2CO_3(aq)$ was added to adjust the pH to 8. The yellow precipitate was set aside and the liquid was decanted and extracted with EtOAc (3×). The combined organic extracts were washed with water (1×) and brine (1×) then dried over $MgSO_4$ and filtered. The solvent was removed under reduced pressure to afford compound **5** (1.48 g, 88%) as a pale yellow solid: mp 132.21 °C; ^{1}H NMR (500 MHz, DMSO-d_6) δ 7.05 (d, $J = 2.4$ Hz, 1H), 6.78 (d, $J = 2.4$ Hz, 1H), 6.69 (dd, $J = 8.2$, 2.5 Hz, 1H), 6.64 (d, $J = 8.1$ Hz, 1H), 6.58 (d, $J = 2.4$ Hz, 1H), 5.24 (s, 2H), 5.11 (s, 2H), 3.48 (s, 3H), 3.41 (s, 3H), 1.78 (s, 3H); ^{13}C{^{1}H} NMR (126 MHz, DMSO-d_6) δ 168.1, 167.3, 147.0, 146.6, 137.3, 131.5, 130.9, 130.5, 129.5, 128.5, 118.1, 117.0, 114.3, 111.7, 51.3, 51.2, 20.5; HRMS (APCI-MS) calcd for $C_{17}H_{19}N_2O_4$ ($[M + H]^+$) 315.1339, found 315.1341.

Dimethyl [1,1'-biphenyl]-4,4'-dihydroxy-6-methyl-2,2'-dicarboxylate (6)

Compound **5** (1.38 g, 4.39 mmol) was dissolved in a mixture of conc. HCl (9.6 mL) and water (48.0 mL). The solution was cooled in an ice bath and an ice-cold mixture of $NaNO_2$ (636 mg, 9.21 mmol) dissolved in water (18.6 mL) was added dropwise while maintaining the temperature between 0–5 °C. The resulting yellow solution was stirred under cold conditions for 10 min. and poured into an ice-cold solution of conc. H_3PO_4 (9.6 mL) in water (700 mL). The resulting light-yellow solution was stirred for 10 min under cold conditions then boiled on a hotplate for 10 min. After cooling the reaction mixture to room temperature, it was extracted with EtOAc (3×) and the combined organic extracts washed with 2 M NaOH(aq) (2×). The aqueous extracts were acidified to pH 4 using conc. HCl and the resulting solution

was extracted with EtOAc (2×). The combined organic extracts were washed with water (1×) and brine (1×), dried over MgSO$_4$, and filtered. The resulting solution was concentrated under reduced pressure and purified on a silica column eluted with 75:25 hexanes:acetone to afford compound **6** (1.00 g, 72%) as a light orange solid: mp 200.63 °C; ^{1}H NMR (500 MHz, DMSO-d_6) δ 9.71 (s, 1H), 9.56 (s, 1H), 7.26 (d, J = 2.7 Hz, 1H), 7.00 (d, J = 2.6 Hz, 1H), 6.94 (dd, J = 8.3, 2.7 Hz, 1H), 6.85–6.80 (m, 2H), 3.50 (s, 3H), 3.43 (s, 3H), 1.82 (s, 3H); ^{13}C{^{1}H} NMR (126 MHz, DMSO-d_6) δ 167.3, 166.6, 155.9, 155.5, 138.2, 132.4, 131.8, 131.5, 130.9, 130.7, 119.8, 118.8, 115.8, 113.0, 51.6, 51.5, 20.4; HRMS (APCI-MS) calcd for C$_{17}$H$_{17}$O$_6$ ([M + H]$^+$) 317.1020, found 317.1021.

Dimethyl [1,1'-biphenyl]-4,4'-bis(3,6,9,12,15,18-hexaoxanonadec-1-yloxy)-6-methyl-2,2'-dicarboxylate (7)

Compound **6** (1.60 g, 5.05 mmol) in dry acetone (90 mL) was treated with K$_2$CO$_3$ (6.97 g, 50.5 mmol) followed by a solution of HxgOTs (6.83 g, 15.17 mmol) in dry acetone (10 mL). The mixture was stirred and heated to reflux overnight under argon, then cooled to room temperature and partitioned between brine and EtOAc. The aqueous layer was extracted with EtOAc (3×) and the combined organic extracts were washed with brine (1×), dried over MgSO$_4$, and filtered. The resulting solution was concentrated under reduced pressure and the crude was purified on a silica column eluted with 70:30 CH$_2$Cl$_2$:acetone to afford the compound **7** (3.23 g, 73%) as a light-yellow oil: ^{1}H NMR (500 MHz, CDCl$_3$) δ 7.56 (d, J = 2.7 Hz, 1H), 7.31 (d, J = 2.7 Hz, 1H), 7.08 (dd, J = 8.4, 2.8 Hz, 1H), 7.01–6.92 (m, 2H), 4.23–4.12 (m, 4H), 3.92–3.82 (m, 4H), 3.78–3.60 (m, 38H), 3.58–3.50 (m, 8H), 3.37 (s, 6H), 1.92 (s, 3H); ^{13}C{^{1}H} NMR (101 MHz, CDCl$_3$) δ 167.7, 167.1, 157.5, 157.1, 138.8, 135.0, 134.3, 131.6, 130.7, 130.6, 120.1, 118.7, 115.4, 112.4, 72.0, 70.92, 70.91, 70.7, 70.65, 70.62, 70.56, 69.76, 69.74, 67.6, 67.5, 59.1, 51.9, 51.85, 20.9; HRMS (APCI-MS) calcd for C$_{43}$H$_{69}$O$_{18}$ ([M + H]$^+$) 873.4478, found 873.4491.

[1,1'-Biphenyl]-4,4'-bis(3,6,9,12,15,18-hexaoxanonadec-1-yloxy)-6-methyl-2,2'-dicarboxylic acid (DP-Ac4)

Compound **7** (2.98 g, 3.43 mmol) in MeOH (50 mL) was treated with NaOH(aq) (2 M, 31 mL, 62 mmol) and the resulting mixture was stirred and heated to reflux overnight. The reaction mixture was concentrated under reduced pressure to remove the methanol and acidified with 2 M HCl(aq) to pH 2. The resulting mixture was saturated with NaCl and extracted with EtOAc (5×) and the combined organic extracts were washed with brine (1×), dried over MgSO$_4$, and filtered. The resulting solution was concentrated under reduced pressure and purified on a silica column eluted with 94:4:1–90:9:1 CH$_2$Cl$_2$:MeOH:AcOH to afford **DP-Ac4** (2.1 g, 73%) as a pale yellow oil: ^{1}H NMR (500 MHz, CDCl$_3$) δ 7.27 (d, J = 2.7 Hz, 1H), 7.07 (d, J = 2.7 Hz, 1H), 6.95 (dd, J = 8.4, 2.7 Hz, 1H), 6.86 (d, J = 8.4 Hz, 1H), 6.82 (d, J = 2.6 Hz, 1H), 4.22–4.01 (m, 4H), 3.88–3.77 (m, 4H), 3.75–3.53 (m, 36H), 3.52–3.45 (m, 4H), 3.32 (s, 6H), 1.82 (s, 3H); ^{13}C{^{1}H} NMR (126 MHz, CDCl$_3$) δ 172.5, 172.0, 157.8, 157.5, 139.2, 135.0, 134.7, 131.9, 131.4, 131.3, 119.0, 117.6, 114.3, 111.5, 71.8, 70.7, 70.52, 70.48, 70.46, 70.42, 70.39, 70.37, 70.3, 69.7, 67.6, 67.5, 59.0, 20.6; HRMS (ESI-MS) calcd for C$_{41}$H$_{64}$O$_{18}$Na ([M + Na]$^+$) 867.3985, found 867.3985.

Dimethyl [1,1'-biphenyl]-6-hydroxy-4,4'-dinitro-2,2'-dicarboxylate (8)

A round-bottomed flask was charged with compound **3** (2.50 g, 5.1 mmol) and Na$_2$CO$_3$ (811 mg, 7.65 mmol) and the mixture treated with EtOH (204 mL). To this mixture was added H$_2$O$_2$ (aq) (30%, 51 mL, 35 mmol) dropwise with stirring. The resulting solution was stirred overnight at room temperature, then the EtOH was removed under reduced pressure. The residue was diluted with water and was extracted with EtOAc (2×). The combined organic extracts were washed with water (1×) and brine (1×), dried over MgSO$_4$, and filtered. The resulting solution was concentrated under reduced pressure and the crude was purified on a silica column eluted with 80:20 hexanes:EtOAc to afford compound **8** (1.18 g, 61%) as a

white solid: mp 235.25 °C; ^{1}H NMR (500 MHz, DMSO-d_6) δ 11.01 (s, 1H), 8.69 (d, J = 2.5 Hz, 1H), 8.45 (dd, J = 8.5, 2.5 Hz, 1H), 8.19 (d, J = 2.3 Hz, 1H), 7.88 (d, J = 2.3 Hz, 1H), 7.50 (d, J = 8.5 Hz, 1H), 3.67 (s, 3H), 3.60 (s, 3H); ^{13}C{^{1}H} NMR (101 MHz, DMSO-d_6) δ 164.7, 164.5, 155.6, 147.4, 146.9, 144.1, 134.9, 132.2, 130.7, 130.6, 126.4, 124.3, 114.8, 112.5, 52.5; HRMS (ESI-MS) calcd for $C_{16}H_{12}N_2O_9Na$ ([M + Na]$^+$) 399.0435, found 399.0436.

Dimethyl [1,1'-biphenyl]-6-methoxy-4,4'-dinitro-2,2'-dicarboxylate (9)

A mixture of compound **8** (2.98 g, 9.13 mmol), K_2CO_3 (6.31 g, 45.66 mmol), methyl iodide (1.14 mL, 18.26 mmol), and dry acetone (94 mL) in a round-bottomed flask was heated to reflux overnight under argon. The reaction mixture was cooled to room temperature and the excess solvent was evaporated under reduced pressure. The residue was diluted with water and extracted with EtOAc (2×). The combined organic extracts were washed with water (1×) and brine (1×), dried over $MgSO_4$, and filtered. The resulting solution was concentrated under reduced pressure and purified on a silica column eluted with 85:15 hexanes:acetone to afford compound **9** (2.75 g, 77%) as a light-yellow solid: mp 160.46 °C; ^{1}H NMR (400 MHz, DMSO-d_6) δ 8.70 (d, J = 2.4 Hz, 1H), 8.46 (dd, J = 8.5, 2.5 Hz, 1H), 8.33 (d, J = 2.1 Hz, 1H), 8.08 (d, J = 2.2 Hz, 1H), 7.51 (d, J = 8.5 Hz, 1H), 3.81 (s, 3H), 3.67 (s, 3H), 3.61 (s, 3H); ^{13}C{^{1}H} NMR (101 MHz, DMSO-d_6) δ 164.5, 164.3, 157.1, 148.0, 147.0, 143.4, 136.4, 132.0, 130.6, 130.4, 126.6, 124.3, 116.4, 109.0, 57.0, 52.64, 52.58; HRMS (ESI-MS) calcd for $C_{17}H_{14}N_2O_9Na$ ([M + Na]$^+$) 413.0592, found 413.0590.

Dimethyl [1,1'-biphenyl]-4,4'-diamino-6-methoxy-2,2'-dicarboxylate (10)

The procedure for compound **5** was followed starting with compound **9** (2.65 g, 6.78 mmol) to afford compound **10** (2.10 g, 94%) as a light-yellow solid: mp 128.91 °C; ^{1}H NMR (400

MHz, DMSO-d_6) δ 7.00 (d, J = 2.0 Hz, 1H), 6.68–6.58 (m, 2H), 6.49 (d, J = 2.1 Hz, 1H), 6.35 (d, J = 2.1 Hz, 1H), 5.26 (s, 2H), 5.19 (s, 2H), 3.55–3.47 (m, 6H), 3.43 (s, 3H); ^{13}C{^{1}H} NMR (101 MHz, DMSO-d_6) δ 168.5, 167.7, 157.2, 148.2, 146.9, 132.02, 131.99, 131.2, 125.1, 118.6, 116.5, 114.3, 106.1, 99.9, 55.1, 51.3, 51.2; HRMS (APCI-MS) calcd for $C_{17}H_{19}N_2O_5$ ([M + H]$^+$) 331.1288, found 331.1291.

Dimethyl [1,1'-biphenyl]-4,4'-dihydroxy-6-methoxy-2,2'-dicarboxylate (11)

The procedure for compound **6** was followed starting with compound **10** (2.00 g, 6.05 mmol) to afford compound **11** (1.14 g, 57%) as an orange solid: mp 206.49 °C; ^{1}H NMR (300 MHz, DMSO-d_6) δ 9.74 (s, 1H), 9.66 (s, 1H), 7.21 (d, J = 2.6 Hz, 1H), 6.88 (dd, J = 8.3, 2.6 Hz, 1H), 6.80 (d, J = 8.3 Hz, 1H), 6.73 (d, J = 2.3 Hz, 1H), 6.57 (d, J = 2.3 Hz, 1H), 3.56 (s, 3H), 3.52 (s, 3H), 3.44 (s, 3H); ^{13}C{^{1}H} NMR (101 MHz, DMSO-d_6) δ 167.6, 166.9, 157.6, 157.0, 155.9, 132.5, 131.7, 131.4, 128.2, 121.7, 118.3, 115.7, 107.2, 102.0, 55.5, 51.6, 51.5; HRMS (APCI-MS) calcd for $C_{17}H_{17}O_7$ ([M + H]$^+$) 333.0969, found 333.0972.

Dimethyl [1,1'-biphenyl]-4,4'-bis(3,6,9,12,15,18-hexaoxanonadec-1-yloxy)-6-methoxy-2,2'-dicarboxylate (12)

The procedure for compound **7** was followed starting with compound **11** (1.08 g, 3.25 mmol) to afford compound **12** (2.37 g, 82%) as a light-yellow oil: ^{1}H NMR (500 MHz, CDCl$_3$) δ 7.53 (d, J = 2.7 Hz, 1H), 7.06 (dd, J = 8.5, 2.8 Hz, 1H), 7.03–6.96 (m, 2H), 6.68 (d, J = 2.5 Hz, 1H), 4.24–4.14 (m, 4H), 3.91–3.85 (m, 4H), 3.77–3.72 (m, 4H), 3.72–3.60 (m, 37H), 3.60–3.51 (m, 8H), 3.37 (s, 6H); ^{13}C{^{1}H} NMR (101 MHz, CDCl$_3$) δ 168.0, 167.4, 158.6, 158.0, 157.6, 132.3, 131.5, 131.4, 130.8, 125.0, 118.3, 115.3, 105.6, 102.8, 72.0, 71.0, 70.9, 70.8, 70.7, 70.68, 70.6, 69.8, 67.7, 67.6, 59.1, 56.1, 52.0, 51.9; HRMS (APCI-MS) calcd for $C_{43}H_{69}O_{19}$ ([M + H]$^+$) 889.4428, found 889.4432.

[1,1'-Biphenyl]-4,4'-bis(3,6,9,12,15,18-hexaoxanonadec-1-yloxy)-6-methoxy-2,2'-dicarboxylic acid (DP-Ac5)

The procedure for compound **DP-Ac4** was followed starting with compound **12** (2.1 g, 2.36 mmol) to afford **DP-Ac5** (1.65 g, 81%) as a light-yellow oil: ^{1}H NMR (500 MHz, CDCl$_3$) δ 7.48 (d, J = 2.7 Hz, 1H), 7.05 (dd, J = 8.4, 2.7 Hz, 1H), 7.02–6.96 (m, 2H), 6.65 (d, J = 2.5 Hz, 1H), 4.27–4.14 (m, 4H), 3.93–3.83 (m, 4H), 3.77–3.69 (m, 4H), 3.69–3.58 (m, 35H), 3.58–3.51 (m, 4H), 3.36 (s, 6H); ^{13}C{^{1}H} NMR (101 MHz, CDCl$_3$) δ 170.74, 170.69, 159.0, 158.3, 157.9, 133.4, 133.1, 132.5, 129.5, 123.1, 118.2, 115.2, 105.4, 102.7, 71.9, 70.93, 70.90, 70.7, 70.64, 70.57, 70.55, 70.52, 70.49, 70.41, 70.38, 69.8, 67.8, 67.7, 59.04, 59.03, 56.1; HRMS (APCI-MS) calcd for C$_{41}$H$_{64}$O$_{19}$Na ([M + Na]$^+$) 883.3934, found 883.3939.

Dimethyl [1,1'-biphenyl]-4,4'-dinitro-6-phenyl-2,2'-dicarboxylate (13)

A dry Schlenk vacuum tube containing compound **2** (3.90 g, 8.88 mmol), Pd(PPh$_3$)$_2$Cl$_2$ (748 mg, 0.12 mmol), phenylbononic acid (2.17 g, 17.76 mmol), and KOAc (3.92 g, 40 mmol) was evacuated and backfilled with argon (3×). To this solid mixture was added dry THF (40 mL). The reaction mixture was degassed by three freeze–pump–thaw cycles and then stirred and heated overnight at 80 °C, cooled to room temperature, and filtered through a Celite pad. The filtrate was diluted with EtOAc, and EtOAc layer was washed with water (3×), sat. NaHCO$_3$ (1×), brine (1×), dried over MgSO$_4$, and filtered. The resulting solution was concentrated under reduced pressure and purified on a silica column eluted with 90:10 cyclohexane:EtOAc to afford compound **13** (2.24 g, 58%) as a white solid: mp 165.95 °C; ^{1}H NMR (500 MHz, DMSO-d_6) δ 8.71 (d, J = 2.4 Hz, 1H), 8.49 (d, J = 2.5 Hz, 1H), 8.34 (d, J = 2.4 Hz, 1H), 8.29 (dd, J = 8.5, 2.5 Hz, 1H), 7.46 (d, J = 8.5 Hz, 1H), 7.27–7.17 (m, 3H), 7.10–7.01 (m, 2H), 3.67 (s, 3H), 3.63 (s, 3H); ^{13}C{^{1}H} NMR (126 MHz, DMSO-d_6) δ 164.8, 164.4, 146.8, 146.6, 145.7, 145.2, 143.0, 137.7, 132.8, 131.1, 130.9, 129.1, 128.2, 128.0, 127.3, 126.0, 123.9, 123.2, 52.8, 52.7; HRMS (ESI-MS) calcd for C$_{22}$H$_{16}$N$_2$O$_8$Na ([M + Na]$^+$)

459.0799, found 459.0796.

Dimethyl [1,1'-biphenyl]-4,4'-diamino-6-phenyl-2,2'-dicarboxylate (14)

The procedure for compound **5** was followed starting with compound **13** (2.28 g, 5.21 mmol) to afford compound **14** (1.65 g, 84%) as a light-yellow solid: mp 212.58 °C; ^{1}H NMR (500 MHz, DMSO-d_6) δ 7.15–7.05 (m, 3H), 7.02–6.95 (m, 2H), 6.88 (d, J = 2.4 Hz, 1H), 6.85 (d, J = 2.4 Hz, 1H), 6.64 (d, J = 2.4 Hz, 1H), 6.47 (d, J = 8.2 Hz, 1H), 6.43 (dd, J = 8.2, 2.4 Hz, 1H), 5.31 (s, 2H), 5.11 (s, 2H), 3.50 (s, 3H), 3.45 (s, 3H); ^{13}C{^{1}H} NMR (126 MHz, DMSO-d_6) δ 168.5, 167.5, 146.8, 146.6, 142.3, 142.0, 132.8, 132.2, 131.3, 129.0, 127.8, 127.7, 127.3, 126.0, 118.0, 116.4, 114.1, 113.0, 51.4, 51.3; HRMS (APCI-MS) calcd for $C_{22}H_{21}N_2O_4$ ([M + H]$^+$) 377.1496, found 377.1498.

Dimethyl [1,1'-biphenyl]-4,4'-dihydroxy-6-phenyl-2,2'-dicarboxylate (15)

The procedure for compound **6** was followed starting with compound **14** (1.52 g, 3.98 mmol) to afford compound **15** (938 mg, 62%) as a light orange solid: mp 208.59 °C; ^{1}H NMR (500 MHz, DMSO-d_6) δ 9.84 (s, 1H), 9.58 (s, 1H), 7.17–7.09 (m, 4H), 7.08–7.03 (m, 1H), 7.01–6.94 (m, 2H), 6.86 (d, J = 2.7 Hz, 1H), 6.69 (d, J = 2.0 Hz, 2H), 3.53 (s, 3H), 3.47 (s, 3H); ^{13}C{^{1}H} NMR (126 MHz, DMSO-d_6) δ 167.6, 166.8, 155.63, 155.57, 143.0, 141.0, 133.2, 132.2, 131.6, 130.8, 130.7, 129.0, 127.5, 126.5, 119.5, 118.1, 115.5, 114.5, 51.7, 51.6; HRMS (APCI-MS) calcd for $C_{22}H_{19}O_6$ ([M + H]$^+$) 379.1176, found 379.1178.

Dimethyl [1,1'-biphenyl]-4,4'-bis(3,6,9,12,15,18-hexaoxanonadec-1-yloxy)-6-phenyl-2,2'-dicarboxylate (16)

The procedure for compound **7** was followed starting with compound **15** (930 mg, 2.45 mmol) to afford compound **16** (1.68 g, 74%) as a colorless oil: ^{1}H NMR (500 MHz, CDCl$_3$) δ 7.42 (d,

J = 2.7 Hz, 1H), 7.33–7.30 (m, 1H), 7.13–7.08 (m, 3H), 7.07 (d, J = 2.7 Hz, 1H), 7.01–6.95 (m, 2H), 6.83 (d, J = 1.5 Hz, 2H), 4.24–4.18 (m, 2H), 4.11–4.05 (m, 2H), 3.91–3.86 (m, 2H), 3.85–3.79 (m, 2H), 3.77–3.49 (m, 46H), 3.37 (s, 6H); $^{13}C\{^1H\}$ NMR (126 MHz, CDCl$_3$) δ 168.1, 167.3, 157.3, 157.25, 143.6, 141.0, 133.42, 133.38, 133.0, 131.9, 131.8, 129.5, 127.7, 126.7, 119.9, 118.0, 114.9, 114.3, 72.1, 71.02, 70.97, 70.8, 70.79, 70.75, 70.72, 70.70, 69.81, 69.79, 67.8, 67.5, 59.2, 52.1, 52.0; HRMS (APCI-MS) calcd for C$_{48}$H$_{71}$O$_{18}$ ([M + H]$^+$) 935.4635, found 935.4629.

[1,1'-Biphenyl]-4,4'-bis(3,6,9,12,15,18-hexaoxanonadec-1-yloxy)-6-phenyl-2,2'-dicarboxylic acid (DP-Ac6)

The procedure for **DP-Ac4** was followed starting with compound **16** (1.38 g, 1.47 mmol) to afford **DP-Ac6** (1.06 g, 72%) as a colorless oil: ^1H NMR (500 MHz, CDCl$_3$) δ 7.39 (d, J = 2.7 Hz, 1H), 7.26–7.24 (m, 1H), 7.14–7.06 (m, 3H), 7.04–6.96 (m, 3H), 6.85–6.75 (m, 2H), 4.24–4.17 (m, 2H), 4.09–4.03 (m, 2H), 3.89–3.83 (m, 2H), 3.81–3.75 (m, 2H), 3.75–3.66 (m, 2H), 3.69–3.55 (m, 34H), 3.56–3.50 (m, 4H), 3.35 (s, 6H); $^{13}C\{^1H\}$ NMR (126 MHz, CDCl$_3$) δ 174.4, 174.3, 157.6, 157.5, 144.4, 141.31, 141.26, 140.0, 132.2, 129.64, 129.59, 129.5, 127.5, 126.5, 117.2, 115.5, 112.7, 112.4, 71.6, 71.4, 70.7, 70.6, 70.22, 70.17, 70.15, 70.12, 70.09, 70.02, 69.98, 69.90, 69.8, 69.7, 69.6, 69.4, 67.6, 67.3, 59.0, 58.9; HRMS (APCI-MS) calcd for C$_{46}$H$_{66}$O$_{18}$Na ([M + Na]$^+$) 929.4141, found 929.4150.

Dimethyl [1,1'-biphenyl]-6-cyano-4,4'-dihydroxy-2,2'-dicarboxylate (17)

A dry Schlenk vacuum tube containing dimethyl [1,1'-biphenyl]-6-bromo-4,4'-dihydroxy-2,2'-dicarboxylate **2** (1.22 g, 3.2 mmol), Pd(dppf)Cl$_2$ (234 mg, 0.32 mmol), and Zn(CN)$_2$ (1.70 g, 9.6 mmol) was evacuated and backfilled with argon (3×). To this solid mixture was added dry DMF (12 mL) and the reaction mixture was degassed by three freeze–pump–thaw cycles

and then stirred and heated overnight at 130 °C, cooled to room temperature, and filtered through a Celite pad. The filtrate was diluted with EtOAc, and EtOAc layer was washed with water (5×), conc. NH_4OH(aq) (2×), brine (1×), dried over $MgSO_4$, and filtered. The resulting solution was concentrated under reduced pressure and purified on a silica column eluted with 70:30 hexane:acetone to afford compound **17** (880 mg, 84%) as a white solid: mp 169.24 °C; ^1H NMR (500 MHz, DMSO-d_6) δ 10.91 (br s, 1H), 10.44 (br s, 1H), 7.91 (d, $J =$ 2.6 Hz, 1H), 7.84–7.73 (m, 2H), 7.49–7.40 (m, 2H), 3.99 (s, 3H), 3.93 (s, 3H); $^{13}C\{^1H\}$ NMR (126 MHz, DMSO-d_6) δ 166.0, 165.6, 157.2, 156.3, 136.5, 132.2, 132.1, 130.3, 129.0, 121.7, 120.5, 119.0, 117.4, 116.4, 114.7, 52.1, 51.9; HRMS (APCI-MS) calcd for $C_{17}H_{14}NO_6$ ([M + H]$^+$) 328.0816, found 328.0819.

Dimethyl [1,1'-biphenyl]-4,4'-bis(3,6,9,12,15,18-hexaoxanonadec-1-yloxy)-6-cyano-2,2'-dicarboxylate (18)

The procedure for compound **7** was followed starting with compound **17** (880 mg, 2.6 mmol) to afford compound **18** (1.70 g, 75%) as a colorless oil: ^1H NMR (500 MHz, CDCl$_3$) δ 7.71 (d, $J =$ 2.7 Hz, 1H), 7.63 (d, $J =$ 2.7 Hz, 1H), 7.35 (d, $J =$ 2.8 Hz, 1H), 7.12 (dd, $J =$ 8.5, 2.7 Hz, 1H), 7.06 (d, $J =$ 8.4 Hz, 1H), 4.25–4.15 (m, 4H), 3.93–3.85 (m, 4H), 3.77–3.70 (m, 4H), 3.70–3.61 (m, 35H), 3.59 (s, 3H), 3.55–3.50 (m, 4H), 3.36 (s, 6H);); $^{13}C\{^1H\}$ NMR (126 MHz, CDCl$_3$) δ 166.4, 165.9, 158.7, 157.5, 139.1, 132.1, 131.6, 131.3, 130.4, 121.3, 120.5, 118.7, 117.3, 116.2, 115.5, 72.0, 71.02, 70.97, 70.74, 70.73, 70.69, 70.68, 70.66, 70.6, 69.7, 69.5, 68.3, 67.7, 59.1, 52.4, 52.2; HRMS (APCI-MS) calcd for $C_{43}H_{66}NO_{18}$ ([M + H]$^+$) 884.4274, found 884.4277.

[1,1'-Biphenyl]-4,4'-bis(3,6,9,12,15,18-hexaoxanonadec-1-yloxy)-6-cyano-2,2'-dicarboxylic acid (DP-Ac7)

Compound **18** (1.13 g, 1.28 mmol) in THF (31 mL) was treated with KOH(aq) (2 M, 10 mL, 20 mmol) and the resulting mixture was stirred and heated to reflux overnight. This was concentrated under reduced pressure to remove THF and acidified with 2 M HCl to pH 2. The resulting mixture was saturated with NaCl, extracted with EtOAc (5×), and the combined organic extracts washed with brine (1×), dried over $MgSO_4$, and filtered. The resulting solution was concentrated under reduced pressure and the crude was purified on a silica column eluted with 94:4:1-89:10:1 CH_2Cl_2:MeOH:AcOH to afford **DP-Ac7** (772 mg, 71%) as a colorless oil: ^1H NMR (400 MHz, $CDCl_3$) δ 7.62 (d, $J = 2.8$ Hz, 1H), 7.53 (s, 1H), 7.28 (d, $J = 2.8$ Hz, 1H), 7.09–6.99 (m, 2H), 4.28–4.10 (m, 4H), 3.93–3.79 (m, 4H), 3.76–3.46 (m, 40H), 3.40–3.26 (m, 6H); $^{13}C\{^1H\}$ NMR (126 MHz, $CDCl_3$) δ 169.6, 168.9, 158.7, 157.7, 137.8, 135.1, 132.9, 131.7, 130.4, 120.9, 119.9, 118.2, 117.4, 116.0, 115.3, 71.9, 71.8, 71.0, 70.8, 70.69, 70.65, 70.58, 70.55, 70.53, 70.50, 70.49, 70.46, 70.43, 70.37, 70.34, 70.32, 70.2, 69.8, 69.7, 68.3, 67.7, 59.08, 59.04; HRMS (ESI-MS) calcd for $C_{41}H_{61}NO_{18}Na$ ($[M + Na]^+$) 878.3781, found 878.3787.

Acknowledgements

References

(1) Mattia, E.; Otto, S. Supramolecular systems chemistry. *Nat. Nanotechnol.* **2015**, *10*, 111–119.

(2) Astumian, R. D. Stochastically pumped adaptation and directional motion of molecular machines. *Proc. Natl. Acad. Sci. U.S.A.* **2018**, *115*, 9405–9413.

(3) Astumian, R. D. Stochastic pumping of non-equilibrium steady-states: how molecules adapt to a fluctuating environment. *Chem. Commun.* **2018**, *54*, 427–444.

(4) Tu, Y.; Rappel, W.-J. Adaptation in living systems. *Annu. Rev. Condens. Matter Phys.* **2018**, *9*, 183–205.

(5) Dinner, A. R.; Blackburn, G. M.; Karplus, M. Uracil-DNA glycosylase acts by substrate autocatalysis. *Nature* **2001**, *413*, 752–755.

(6) Mulder, B. M.; Janson, M. E. Self-healing microtubules. *Nature Mater.* **2015**, *14*, 1080–1081.

(7) Alberts, B.; Johnson, A.; Lewis, J.; Morgan, D.; Raff, M.; Roberts, K.; Walter, P., *Molecular Biology of the Cell*, 6th ed.; W. W. Norton & Company: New York, 2015.

(8) Ashkenasy, G.; Hermans, T. M.; Otto, S.; Taylor, A. F. Systems chemistry. *Chem. Soc. Rev.* **2017**, *46*, 2543–2554.

(9) Weißenfels, M.; Gemen, J.; Klajn, R. Dissipative self-assembly: Fueling with chemicals versus light. *Chem* **2021**, *7*, 23–37.

(10) Patel, S. S.; Pandey, M.; Nandakumar, D. Dynamic coupling between the motors of DNA replication: hexameric helicase, DNA polymerase, and primase. *Curr. Opin. Chem. Biol.* **2011**, *15*, 595–605.

(11) Goshima, G.; Vale, R. D. The roles of microtubule-based motor proteins in mitosis: comprehensive RNAi analysis in the *Drosophila* S2 cell line. *J. Cell. Biol.* **2003**, *162*, 1003–1016.

(12) Fourriere, L.; Jimenez, A. J.; Perez, F.; Boncompain, G. The role of microtubules in secretory protein transport. *J. Cell Sci.* **2020**, *133*, jcs237016.

(13) Klopfenstein, D. R.; Vale, R. D.; Rogers, S. L. Motor protein receptors: Moonlighting on other jobs. *Cell* **2000**, *103*, 537–540.

(14) Dawson, R. J. P.; Locher, K. P. Structure of a bacterial multidrug ABC transporter. *Nature* **2006**, *443*, 180–185.

(15) Kariyawasam, L. S.; Hossain, M. M.; Hartley, C. S. The transient covalent bond in abiotic nonequilibrium systems. *Angew. Chem., Int. Ed.* **2021**, *60*, 12648–12658.

(16) Sorrenti, A.; Leira-Iglesias, J.; Markvoort, A. J.; De Greef, T. F. A.; Hermans, T. M. Non-equilibrium supramolecular polymerization. *Chem. Soc. Rev.* **2017**, *46*, 5476–5490.

(17) van Rossum, S. A. P.; Tena-Solsona, M.; van Esch, J. H.; Eelkema, R.; Boekhoven, J. Dissipative out-of-equilibrium assembly of man-made supramolecular materials. *Chem. Soc. Rev.* **2017**, *46*, 5519–5535.

(18) Tena-Solsona, M.; Wanzke, C.; Riess, B.; Bausch, A. R.; Boekhoven, J. Self-selection of dissipative assemblies driven by primitive chemical reaction networks. *Nat. Commun.* **2018**, *9*, 2044.

(19) Dai, K.; Fores, J. R.; Wanzke, C.; Winkeljann, B.; Bergmann, A. M.; Lieleg, O.; Boekhoven, J. Regulating chemically fueled peptide assemblies by molecular design. *J. Am. Chem. Soc.* **2020**, *142*, 14142–14149.

(20) Späth, F.; Donau, C.; Bergmann, A. M.; Kränzlein, M.; Synatschke, C. V.; Rieger, B.; Boekhoven, J. Molecular design of chemically fueled peptide–polyelectrolyte coacervate-based assemblies. *J. Am. Chem. Soc.* **2021**, *143*, 4782–4789.

(21) Zhang, B.; Jayalath, I. M.; Ke, J.; Sparks, J. L.; Hartley, C. S.; Konkolewicz, D. Chemically fueled covalent crosslinking of polymer materials. *Chem. Commun.* **2019**, *55*, 2086–2089.

(22) Kariyawasam, L. S.; Kron, J. C.; Jiang, R.; Sommer, A. J.; Hartley, C. S. Structure–property effects in the generation of transient aqueous benzoic acid anhydrides by carbodiimide fuels. *J. Org. Chem.* **2020**, *85*, 682–690.

(23) Hossain, M. M.; Atkinson, J. L.; Hartley, C. S. Dissipative assembly of macrocycles comprising multiple transient bonds. *Angew. Chem., Int. Ed.* **2020**, *59*, 13807–13813.

(24) Bal, S.; Ghosh, C.; Ghosh, T.; Vijayaraghavan, R. K.; Das, D. Non-equilibrium polymerization of cross-β amyloid peptides for temporal control of electronic properties. *Angew. Chem., Int. Ed.* **2020**, *59*, 13506–13510.

(25) Bal, S.; Das, K.; Ahmed, S.; Das, D. Chemically fueled dissipative self-assembly that exploits cooperative catalysis. *Angew. Chem., Int. Ed.* **2019**, *58*, 244–247.

(26) Bai, S.; Niu, X.; Wang, H.; Wei, L.; Liu, L.; Liu, X.; Eelkema, R.; Guo, X.; van Esch, J. H.; Wang, Y. Chemical reaction powered transient polymer hydrogels for controlled formation and free release of pharmaceutical crystals. *Chem. Eng. J. (Amsterdam, Neth.)* **2021**, *414*, 128877.

(27) Heckel, J.; Loescher, S.; Mathers, R. T.; Walther, A. Chemically fueled volume phase transition of polyacid microgels. *Angew. Chem., Int. Ed.* **2021**, *60*, 7117–7125.

(28) Borsley, S.; Leigh, D. A.; Roberts, B. M. W. A doubly kinetically-gated information ratchet autonomously driven by carbodiimide hydration. *J. Am. Chem. Soc.* **2021**, *143*, 4414–4420.

(29) Jayalath, I. M.; Wang, H.; Mantel, G.; Kariyawasam, L. S.; Hartley, C. S. Chemically fueled transient geometry changes in diphenic acids. *Org. Lett.* **2020**, *22*, 7567–7571.

(30) Efforts to incorporate isopropyl and *tert*-butyl substituents at the 6 position of diphenic acids were unsuccessful as the Suzuki reaction did not yield the corresponding products.

(31) Kariyawasam, L. S.; Hartley, C. S. Dissipative assembly of aqueous carboxylic acid anhydrides fueled by carbodiimides. *J. Am. Chem. Soc.* **2017**, *139*, 11949–11955.

(32) DeTar, D. F.; Silverstein, R. Reactions of carbodiimides. I. The mechanisms of the reactions of acetic acid with dicyclohexylcarbodiimide. *J. Am. Chem. Soc.* **1966**, *88*, 1013–1019.

(33) Williams, A.; Ibrahim, I. T. Carbodiimide chemistry: recent advances. *Chem. Rev.* **1981**, *81*, 589–636.

(34) Iwasawa, T.; Wash, P.; Gibson, C.; Rebek Jr., J. Reaction of an introverted carboxylic acid with carbodiimide. *Tetrahedron* **2007**, *63*, 6506–6511.

(35) Butler, A. R.; Gold, V. 859. The hydrolysis of acetic anhydride. Part VII. Catalysis by pyridine and methylpyridines in acetate buffers. *J. Chem. Soc.* **1961**, 4362–4367.

(36) Fersht, A. R.; Jencks, W. P. The acetylpyridinium ion intermediate in pyridine-catalyzed hydrolysis and acyl transfer reactions of acetic anhydride. Observation, kinetics, structure–reactivity correlations, and effects of concentrated salt solutions. *J. Am. Chem. Soc.* **1970**, *92*, 5432–5442.

(37) Ibrahim, I. T.; Williams, A. Reaction of the water-soluble reagent *N*-ethyl-*N'*-(3-dimethylaminopropyl)carbodiimide with nucleophiles: participation of the tautomeric cyclic ammonioamidine as a kinetically important intermediate. *J. Am. Chem. Soc.* **1978**, *100*, 7420–7421.

(38) Johnson, K. A.; Simpson, Z. B.; Blom, T. FitSpace Explorer: An algorithm to evaluate multidimensional parameter space in fitting kinetic data. *Anal. Biochem.* **2009**, *387*, 30–41.

(39) Hansch, C.; Leo, A; Taft, R. W. A survey of Hammett substituent constants and resonance and field parameters. *Chem. Rev.* **1991**, *91*, 165–195.

(40) We tried plotting the parameters vs σ_p instead, so as to see the effect of conjugation of the other carbonyl via the biaryl bond (see Supporting Information). However, the correlations did not improve.

(41) Berliner, E.; Altschul, L. H. The hydrolysis of substituted benzoic anhydrides. *J. Am. Chem. Soc.* **1952**, *74*, 4110–4113.

(42) Meiners, F.; Ross, J. H.; Brand, I.; Buling, A.; Neumann, M.; Köster, P. J.; Christoffers, J.; Wittstock, G. Modification of silicon oxide surfaces by monolayers of an oligoethylene glycol-terminated perfluoroalkyl silane. *Colloids Surf., A* **2014**, *449*, 31–41.